Energy & Environmental Science

Cite this: *Energy Environ. Sci.*, 2012, **5**, 6089

www.rsc.org/ees

PAPER

Influence of the counter electrode on the photovoltaic performance of dye-sensitized solar cells using a disulfide/thiolate redox electrolyte

Julian Burschka,[a] Vincent Brault,[b] Shahzada Ahmad,[ac] Livain Breau,[b] Mohammad K. Nazeeruddin,[a] Benoît Marsan,*[b] Shaik M. Zakeeruddin*[a] and Michael Grätzel*[a]

Received 27th October 2011, Accepted 16th December 2011
DOI: 10.1039/c2ee03005e

Strong scientific interests focus on the investigation of iodine-free redox couples for their application in dye-sensitized solar cells (DSCs). Recently, a disulfide/thiolate-based redox electrolyte has been proposed as a valuable alternative to the conventional I_3^-/I^- system due to its transparent and non-corrosive nature. In the work presented herein, we systematically studied the influence of different counter electrode materials on the photovoltaic performance of DSCs employing this promising organic redox electrolyte. Our investigations focused on understanding the importance of electrocatalytic activity and surface area of the electroactive material on the counter electrode, comparing the conventional platinum to cobalt sulfide (CoS) and poly(3,4-ethylenedioxythiophene) (PEDOT). Electrochemical Impedance Spectroscopy has been used to study in detail the interfacial charge transfer reaction at the counter electrode. By using a high surface area PEDOT-based counter electrode, we finally achieved an unprecedented power conversion efficiency of 7.9% under simulated AM1.5G solar irradiation (100 mW cm^{-2}) which, to the best of our knowledge, represents the highest efficiency that has so far been reported for an organic redox couple.

1. Introduction

The development of sustainable energies that do not rely on fossil fuels is a key objective of modern research. Strong endeavours focus on the conversion of solar energy into electricity and especially on finding alternatives to conventional silicon-based photovoltaic cells. Among those so-called third generation photovoltaic devices, dye-sensitized solar cells (DSCs) gained notable importance, primarily due to their high light-to-electricity conversion efficiency, low production costs and an eco-friendly nature.[1]

[a]*Laboratory for Photonics and Interfaces, Swiss Federal Institute of Technology, CH 1015 Lausanne, Switzerland. E-mail: michael.graetzel@epfl.ch; shaik.zakeer@epfl.ch*
[b]*Département de chimie, Université du Québec à Montréal, C.P. 8888, Succ. Centre-ville, Montréal, QC, Canada H3C 3P8. E-mail: marsan.benoit@uqam.ca*
[c]*Max Planck Institute for Polymer Research, Ackermannweg 10, D-55128 Mainz, Germany*

Broader context

A constantly increasing world energy consumption, the inevitable depletion of fossil fuel and global warming caused by excessive emission of greenhouse gases demand the development of alternative, sustainable energy sources. Besides biomass, wind and hydropower, solar energy is seen as one of the top candidates to resolve world's energy crisis. Although photovoltaic devices that can efficiently convert solar energy into electricity have been developed many years ago, the final breakthrough is retarded by reasons of high costs and energy consumption during the fabrication process of conventional silicon-based solar cells. However, during the last few decades cost-efficient and promising alternatives based on organic materials have been proposed, amongst them is the dye-sensitized solar cell (DSC) imitating Nature's amazing energy conversion machinery—the photosynthesis. Since its development twenty years ago, the DSC technology has been relying on the I_3^-/I^- redox couple as a mediator for oxidized dye regeneration, although several disadvantageous properties of the redox active species warrant a suitable alternative. Herein, we focus on a new organic redox couple and combine it with two inexpensive and abundant counter electrode materials—poly(3,4-ethylenedioxythiophene) (PEDOT) and cobalt(II)sulfide—in order to pave the way for a clean and eco-friendly solar energy conversion device.

The most widely employed mediator responsible for oxidized-dye-regeneration in DSCs is the I_3^-/I^- couple that has been the redox system of choice since DSC development.[2] However, corrosion, absorption of visible light and an inappropriate redox potential that leads to low open-circuit voltages, demand the design of new suitable alternatives.[3] During the last few decades, many redox-active compounds have been proposed,[4] but only recently, efficiencies over 6% could be achieved employing iodine-free redox electrolytes in DSCs. Thus, one-electron outer-sphere redox couples based on metal–organic complexes of $Co^{III/II}$ or $Fe^{I/0}$ yielded overall power conversion efficiencies (PCE) up to 9.6% and 7.5%, respectively.[5,6]

In this context, Wang *et al.* reported on an organic disulfide/thiolate redox couple, 5,5′-dithiobis(1-methyltetrazole)/1-methyltetrazole-5-thiolate (T_2/T^-), that shows almost no absorption of visible light and achieving 6.4% PCE under simulated Air Mass (AM) 1.5 global (G) solar irradiance (100 mW cm^{-2}).[7] As reported, one of the major drawbacks when using this redox system was a relatively low fill factor (FF) of approximately 0.60. More recently, two other organic redox couples noted BMT/McMT$^-$ (2,2′dithiobis(5-methyl-1,3,4-thiadiazole)/5-methyl-1,3,4-thiadiazole-2-thiolate) and $TMFDS^{2+}$/TMTU (dithiobis-(*N*,*N*,*N*′,*N*′-tetramethylformamidinium)/*N*,*N*,*N*′,*N*′-tetramethylthiourea) have been investigated as redox shuttles for dye solar cells.[8,9] The structures of the oxidized and reduced species of all three organic redox couples are depicted in Fig. 1. In the case of the BMT/McMT$^-$ redox couple, a PCE of 4.0% was reached, though the fill factor of the corresponding photovoltaic device was only 0.42. For the $TMFDS^{2+}$/TMTU redox couple, obtained fill factors were below 0.30, but this value was significantly improved by replacing the electroactive platinum layer on the counter electrode by a carbon-based material. More recently, Wu *et al.* proposed molybdenum sulfide (MoS_2) and tungsten sulfide (WS_2) as viable counter electrode catalysts for triiodide-to-iodide as well as disulfide-to-thiolate reduction in DSCs and one could observe a significant improvement in FF in the latter case.[10]

The phenomenon of a low fill factor with sulfur-functionalized redox mediators is most likely to result from slow catalytic reduction of the oxidized species at the standard platinum-loaded counter electrode. The slow electron transfer leads to a high interfacial charge transfer resistance limiting the fill factor of the device.[11] Therefore, alternative electrocatalysts that exhibit fast electron transfer kinetics for the disulfide-to-thiolate reduction and reasonable stability towards the above-mentioned redox couples have to be explored.

Since the early days of DSCs, significant efforts have been spent in order to develop alternative and in particular noble-metal-free counter electrodes. Especially for practical large-scale applications, it is required to replace the expensive platinum by a cheaper and abundant counter electrode material in order to make the DSC technology cost-effective.[12] In this context, electrocatalysts ranging from carbon-based materials, such as carbon black,[13] carbon nanotubes[14] or graphene,[15] to inorganic compounds, such as transition metal sulfides,[16] nitrides[17] or carbides,[18] and conducting polymers, such as polyaniline,[19] polypyrrole[20] or poly(3,4-ethylenedioxythiophene)[21] (PEDOT), have been investigated.

PEDOT is a well-known conductive polymer with numerous applications that is extensively used, for instance as a buffer layer in organic light-emitting diodes, oxygen reduction catalyst or antistatic coating.[22] PEDOT is usually deposited from a commercially available aqueous dispersion of PEDOT, stabilized with poly(styrenesulfonate) (PSS), that can be applied by any of the wet chemistry methods such as spin-coating or doctor-blading to yield transparent thin films of good chemical and electrochemical stability.[23] However, the conductivity of bare PEDOT:PSS is too low for the application in DSCs and reasonable efficiencies can only be achieved when the polymer film is further modified.[21a] By contrast, direct chemical or electrochemical polymerization of ethylenedioxythiophene (EDOT) on transparent conductive substrates (TCO) has been proved to be a promising technique to yield PEDOT films of good conductivity and electrocatalytic activity.[21b,c] Remarkable performances could be achieved when PEDOT-based counter electrodes were prepared by electropolymerization of the EDOT monomer in hydrophobic ionic-liquid medium.[24] This method results in the formation of a highly porous structured polymer film with high catalytic activity and surface area. The nature of the employed ionic liquid used as a medium for the polymerization has a strong influence on the morphology of the polymer film that is highly conductive due to intrinsic doping. As a matter of fact, both the anion and cation of the employed ionic liquid are incorporated into the polymer film.[25] When this article was ready for submission, a parallel work appeared, investigating PEDOT-based counter electrodes grown in classical salt and solvent medium for several disulfide/thiolate redox electrolytes finally reaching a PCE of 6.0% with the BMT/McMT$^-$ redox couple and an organic sensitizer.[26] However, the desired microstructure and long term stability of PEDOT cannot be attended when grown in classical electrolyte media.

Herein we report on the feasibility of two platinum-free counter electrodes, namely cobalt sulfide (CoS) and PEDOT, for disulfide-to-thiolate reduction in DSCs by studying and understanding their electrocatalytic activity in combination with the promising T_2/T^- redox couple. Both of the materials have recently been proven as valuable alternatives to platinized counter electrodes for triiodide-to-iodide reduction in DSCs and are of particular interest due to lower costs, ease of fabrication and comparable device performance.[16a,24]

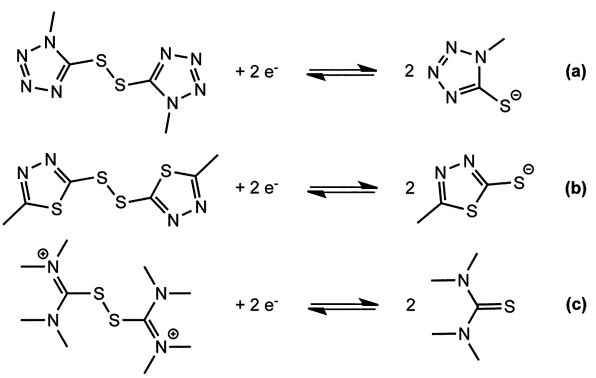

Fig. 1 Structures of sulfur-functionalized redox couples: (a) T_2/T^-, (b) BMT/McMT$^-$ and (c) $TMFDS^{2+}$/TMTU.

2. Experimental details

All chemicals were obtained from Sigma-Aldrich (Switzerland or Canada) and used without further purification unless otherwise stated. Ethylene carbonate and 3-methoxypropionitrile were purified by distillation. The ionic liquid 1-ethyl-3-methylimidazolium tris(pentafluoroethyl)trifluorophosphate (EMI-FAP) and iodine were purchased from Merck KGaA (Germany) and used as received. The Z907 sensitizer, 1,3-dimethylimidazolium iodide as well as the oxidized and reduced species of the employed redox couple 1-methyltetrazole-5-thiolate (T^-) and 5,5′-dithiobis(1-methyltetrazole) (T_2) were synthesized as previously reported.[7,27,28] Only a small change was made for the synthesis of the thiolate salt. In this work, we used equimolar quantities of 5-mercapto-1-methyltetrazole (1.46 g, 12.6 mmol) and tetramethylammonium hydroxide (5.8 mL of the 25 wt% solution in methanol, 12.6 mmol) to neutralize the thiol.

2.1 Preparation of PEDOT counter electrodes

PEDOT was deposited on conductive substrates by electropolymerization in a three-electrode configuration cell. Thus, TCO substrates, connected as working electrode, were immersed vertically into the ionic-liquid polymerization medium (EMI-FAP) containing 0.1 M EDOT monomer, whereas a platinum rod and a leak-free Ag/AgCl electrode were used as counter and reference electrodes, respectively. The polymer films were grown potentiostatically at a DC potential of 1.2 V supplied by an Autolab PGSTAT 30 (Metrohm) for the duration of 30 s. The PEDOT electrodes were subsequently washed with 2-propanol and dried under dry air flow. PEDOT films deposited on standard fluorine-doped tin oxide (FTO) coated glass (Tec 15, Pilkington) as well as on indium tin oxide (ITO) coated flexible polyethyleneterephthalate (PET) substrates (OIKE Co., Ltd.) have been studied. The substrates were cleaned by ultrasonication in water and ethanol, and dried under air stream prior to their use.

2.2 Preparation of CoS counter electrodes

CoS was electrodeposited at 22 °C, on a 4 cm^2 ITO coated flexible PEN substrate previously cleaned by ultrasonication in acetone followed by drying under air stream, using a one-compartment glass cell with a three-electrode configuration, as previously reported.[16a] The deposition bath was an alkaline (pH = 10) aqueous solution containing 5 mM cobalt(II) chloride hexahydrate and 150 mM thiourea. A 1.5 cm^2 Pt gauze served as the counter electrode and an Ag/AgCl/NaCl 3 M electrode was used as the reference. The potentiostatic deposition was carried out at a DC potential of −0.8 V for the duration of 30 min. A multipotentiostat (Solartron Instruments, model 1470) interfaced with a PC was employed for the depositions that were controlled with the CorrWare2 software (Scribners Associates, version 2.80c).

2.3 Preparation of Pt counter electrodes

Platinum-based counter electrodes were fabricated by drop-casting a 7 mM solution of H_2PtCl_6 in 2-propanol on FTO coated glass substrates (TEC 15). The substrates were subsequently heated to 410 °C during 15 min to yield semi-transparent platinized counter electrodes that were used without any further treatment.

2.4 Fabrication of photovoltaic devices

FTO coated glass substrates (Solar 4 mm, Nippon Sheet Glass) were first treated in a 40 mM aqueous $TiCl_4$ solution at 70 °C for 30 min, rinsed with deionized water and dried at 450 °C for 30 min. TiO_2 nanoparticles were subsequently deposited on the substrates by a screen printing technique and dried at 125 °C for 8 min. After repeating this step several times until the desired film thickness was reached, the mesoporous films were gradually heated to 500 °C and sintered at this temperature for 20 min. TiO_2 films employed in this study were composed of an 8 μm thick transparent layer (20 nm particle diameter) and a 5 μm thick scattering layer (400 nm particle diameter). Afterwards, the substrates were again treated in a 40 mM aqueous $TiCl_4$ solution at 70 °C for 30 min. Prior to sensitization, the mesoporous films were heated to 450 °C for 30 min. After cooling down to approximately 60 °C, a 7 mM solution of the Z907 sensitizer in *N*,*N*-dimethylformamide (DMF) was drop-cast on the films, left for 10 min and the excess solution was removed by rinsing with acetonitrile. The sensitized photoanodes were assembled with different counter electrodes using a 25 μm thick hot-melting polymer spacer (Surlyn, DuPont) before injecting the electrolyte through a hole in the counter electrode with the aid of a vacuum backfilling system. The hole was subsequently sealed with a polymer sheet (Surlyn, DuPont) and a microscopic coverslide. The electrolyte that has been used for the comparison of different counter electrode materials was composed of 0.4 M T_2 and 0.4 M T^- (tetramethylammonium salt) in 3-methoxypropionitrile (MPN). Additionally, a volatile electrolyte composed of 0.3 M T_2 and 0.9 M T^- (tetramethylammonium salt) in a mixture of acetonitrile/ethylene carbonate (6 : 4 volume ratio) has been studied.

2.5 Photovoltaic characterization

For the photovoltaic measurements, devices were equipped with a UV cut-off filter and masked with a thin metal mask to give an active area of 0.159 cm^2. *J*–*V* characteristics were recorded by applying an external potential bias to the cell while measuring the current response with a Keithley 2400 SourceMeter (Keithley). The light source was a 450 W xenon lamp (Oriel) equipped with a Schott K113 Tempax filter in order to match the emission spectrum of the lamp to the AM1.5G standard. Incident photon-to-electron conversion efficiency (IPCE) spectra were recorded with a Keithley 2400 SourceMeter (Keithley) as a function of wavelength under a constant white light bias of approximately 5 mW cm^{-2} supplied by a white LED array. The excitation beam coming from a 300 W xenon lamp (ILC Technology) was focused through a Gemini-180 double monochromator (Jobin Yvon Ltd.) and chopped at approximately 4 Hz.

2.6 Stability tests

For stability tests under ambient conditions, the devices were stored at room temperature under the exclusion of light. For stability tests under standard test conditions (60 °C, 100 mW cm^{-2} AM1.5G), the devices were kept in a solar simulator

equipped with a Sun test CPS+ lamp (ATLAS). In both cases, *J–V* characteristics were measured every week to follow the changes with aging time.

2.7 Electrochemical Impedance Spectroscopy (EIS)

EIS spectra were recorded using symmetrical thin-layer cells (SC) composed of two identical electrodes separated by the electrolyte. The polymer spacer used in this case (Surlyn, DuPont) was 50 μm thick and the electrolyte was injected using the same aforementioned vacuum backfilling process. EIS measurements were carried out using an Autolab Frequency Response Analyzer (PGSTAT 30, Metrohm) at 0 V DC bias potential (simulated open-circuit conditions) for frequencies ranging from 1 MHz to 100 mHz. The experimental data were fitted using an equivalent circuit composed of an ohmic series resistance (R_s) and an RC-element. The charge transfer resistance (R_{ct}) was calculated as half the value obtained from the EIS fitting (the cells used were symmetric) multiplied by the geometric surface area of the electrode. In the case of the PEDOT|FTO|Glass electrode, a second semicircle appearing at high frequency was observed and that has been considered during the fitting in the form of a second RC element. Warburg impedance appearing in the low frequency range was observed only in the case of the I_3^-/I^-|Pt system. The disulfide/thiolate redox electrolyte that has been used for the EIS characterization was the same MPN-based electrolyte as in the case of complete photovoltaic devices. The electrolyte used for the I_3^-/I^- reference was composed of 0.4 M I_2 and 0.8 M 1,3-dimethylimidazolium iodide (DMII) in MPN. The active surface area of the symmetrical cells was 0.3949 cm^2.

3. Results and discussion

3.1 Photovoltaic performance

The photovoltaic performance of alternative counter electrodes based on CoS and PEDOT was evaluated by fabricating nanocrystalline dye-sensitized solar cells using the ruthenium-based Z907 sensitizer and the T_2/T^- organic redox couple in 3-methoxypropionitrile (MPN) solvent. *J–V* characteristics measured under simulated AM1.5G solar irradiance (100 mW cm^{-2}) are shown in Fig. 2 and detailed photovoltaic parameters at different light intensities are given in Table 1. Under full sun illumination, the photovoltaic parameters, fill factor (FF), short-circuit current density (J_{SC}) and open-circuit potential (V_{OC}), of the reference device containing the conventional platinum-loaded counter electrode (Device A) are 0.59, 15.1 mA cm^{-2} and 633 mV, respectively, yielding an overall power conversion efficiency (η) of 5.6%. A remarkably high fill factor of 0.70 is obtained when using PEDOT on FTO glass as a counter electrode (Device B), leading to an impressive overall power conversion efficiency of 6.9%. The efficiency drops to 5.9% when PEDOT is deposited on a flexible ITO|PET substrate (Device D) due to a lower fill factor. This effect can be partly attributed to the higher sheet resistance of the ITO|PET substrate (30–50 Ω sq^{-1}) compared to standard FTO glass (15 Ω sq^{-1}). The CoS counter electrode (Device C) yields a relatively low fill factor of 0.49 at full sunlight intensity, resulting from an S-shaped *J–V* curve. However, a reasonable power conversion efficiency of 6.6% is obtained at low light intensity, a value that is in accordance with the PEDOT on a flexible ITO|PET device. In general, *J–V* characteristics show that it is mainly the fill factor of the cells that is affected by the change of the electroactive material at the counter electrode. For all the four devices A to D, an open-circuit potential of approximately 637 ± 5 mV was obtained. However, the short-circuit current density found for devices employing flexible counter electrodes (devices C and D) is slightly lower than the one achieved with counter electrodes based on standard FTO glass (devices A and B). The reason for this phenomenon is still unclear as these materials are non-reflective and current dynamics show that the J_{SC} is not limited by a slow disulfide-to-thiolate reduction process at the counter electrode. Under those conditions a difference in J_{SC} is not expected.

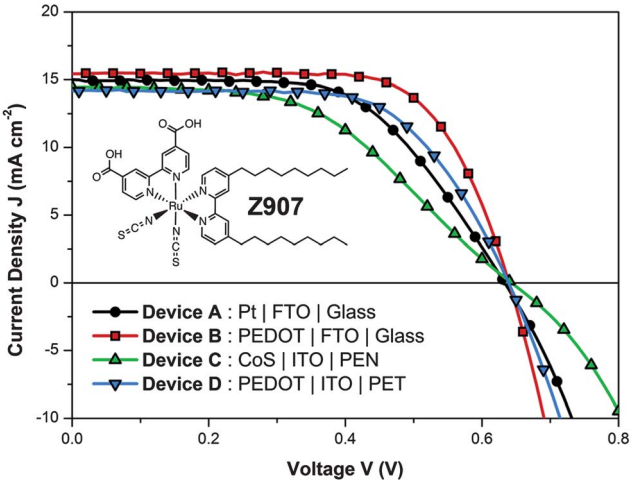

Fig. 2 *J–V* characteristics of photovoltaic devices prepared with different counter electrodes measured under 100 mW cm^{-2} illumination (solid lines) and in the dark (dashed lines). Device A: Pt|FTO|Glass. Device B: PEDOT|FTO|Glass. Device C: CoS|ITO|PEN. Device D: PEDOT|ITO|PET. The electrolyte is 0.4 M T_2 and 0.4 M T^- in 3-methoxypropionitrile, the TiO_2 film thickness is 8 + 5 μm. The inset depicts the structure of the employed amphiphilic ruthenium sensitizer Z907.

3.2 Characterization by Electrochemical Impedance Spectroscopy

Electrochemical Impedance Spectroscopy (EIS) has been used to study further the interfacial charge transfer reaction at the counter electrode employing symmetrical thin-layer cells (SC) composed of two identical electrodes sandwiched together with the redox electrolyte filling the space in-between. Nyquist plots at 20 °C for the different counter electrode materials are shown in Fig. 3. Data for a device employing the conventional I_3^-/I^- redox couple and a platinized counter electrode are also shown for comparison.

As the investigated devices are symmetrical, a Nyquist plot composed of two components is expected:[29] firstly, a semicircle appearing at high frequency due to the charge transfer at the electrode|electrolyte interface from which the charge transfer resistance R_{ct} can be derived and secondly, a Warburg impedance caused by ion diffusion through the bulk electrolyte in the lower frequency range. This ideal spectrum is solely observed in the

Table 1 Detailed photovoltaic parameters measured at different incident light intensities (AM1.5G Standard)

	Device A			Device B			Device C			Device D		
	Pt|FTO|Glass			PEDOT|FTO|Glass			CoS|ITO|PEN			PEDOT|ITO|PET		
Intensity/mW cm^{-2}	10	50	100	10	50	100	10	50	100	10	50	100
V_{OC}/mV	583	620	633	580	624	639	595	631	643	582	624	639
J_{SC}/mA cm^{-2}	1.6	7.8	15.1	1.6	7.9	15.5	1.5	7.5	14.6	1.5	7.3	14.2
FF	0.75	0.66	0.59	0.78	0.74	0.70	0.72	0.57	0.49	0.76	0.70	0.65
η (%)	7.0	6.4	5.6	7.3	7.3	6.9	6.6	5.4	4.6	6.5	6.4	5.9

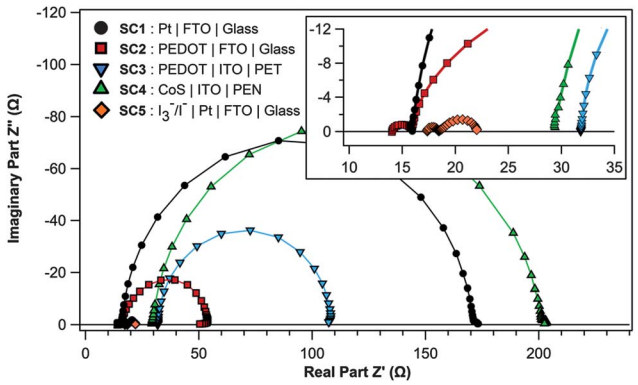

Fig. 3 Nyquist plots at 0 V bias potential and 20 °C obtained for symmetrical cells fabricated using different counter electrodes: SC1: Pt|FTO|Glass, SC2: PEDOT|FTO|Glass, SC3: PEDOT|ITO|PET, SC4: CoS|ITO|PEN, and SC5: I_3^-/I^-|Pt|FTO|Glass. The electrolyte for the cells SC1 to SC4 is the same as in Fig. 2. The electrolyte used for the cell SC5 is composed of 0.4 M I_2 and 0.8 M dimethylimidazolium iodide (DMII) in 3-methoxypropionitrile as a solvent. The active area of the cells was 0.3949 cm^2.

case of the I_3^-/I^-|Pt system. For the disulfide/thiolate electrolyte, the Warburg impedance only becomes visible at high bias potentials (data not shown). In the case of the PEDOT|FTO|Glass electrode, a second semicircle, that probably results from charge transfer at the PEDOT|FTO interface, appears at high frequency. From the Nyquist plot, it can be seen that the series resistance (R_s) in the case of the flexible substrate electrodes is about twice as large as that of standard FTO glass, an effect that is due to the difference in sheet resistance. The corresponding values are 15 Ω sq^{-1} for FTO glass and about 30–50 Ω sq^{-1} for the ITO|PET and ITO|PEN substrates. At 20 °C, a relatively low charge transfer resistance of 7.8 Ω cm^2 for the thiolate/disulfide-based electrolyte is achieved when the PEDOT|FTO|Glass counter electrode (SC2) was used compared to 30.5 Ω cm^2 with platinum (SC1). The corresponding values for CoS (SC4) and PEDOT (SC3) on flexible substrates are 33.8 Ω cm^2 and 15.2 Ω cm^2, respectively.

The derived charge transfer resistances for the different electroactive materials basically correlate with the fill factors and power conversion efficiencies calculated from *J–V* measurements of photovoltaic devices. It is observed that the charge transfer resistance obtained for the disulfide/thiolate-based electrolyte and the best performing electrocatalyst is still much higher than the value obtained for the triiodide-to-iodide reduction on the platinum counter electrode (SC5). In the latter case, a charge transfer resistance of only 0.2 Ω cm^2 is reached. Values that can be found in the literature usually lie in the range of 1 Ω cm^2.[29] However, it has to be noted that the employed I_3^-/I^- electrolyte contains the same concentrations of oxidized and reduced species as the disulfide/thiolate electrolyte used herein, which do not correspond to what is generally used for I_3^-/I^- based photovoltaic devices.

In order to get more information about the kinetics of the charge transfer reaction, EIS measurements have been conducted at different temperatures ranging from −15 °C to 35 °C. Fig. 4 depicts the R_{ct} values as a function of the inverse of the absolute temperature. From the charge transfer resistance, the exchange current density (J_0) can be calculated by using

$$J_0 = RT/nFR_{ct} \quad (1)$$

where R is the gas constant, T the absolute temperature, n the number of electrons being transferred during the disulfide-to-thiolate reduction process and F the Faraday constant. J_0 is an important parameter describing the kinetics of the charge transfer reaction at the electrode|electrolyte interface. The exchange current density follows the Arrhenius equation

$$J_0 = J_{inf}e^{-Ea/RT} \quad (2)$$

where J_{inf} is the exchange current density at infinite temperature and E_a is the apparent activation energy. The corresponding Arrhenius plots are shown in Fig. 5. Following eqn (2), the temperature-dependent measurements enable the calculation of

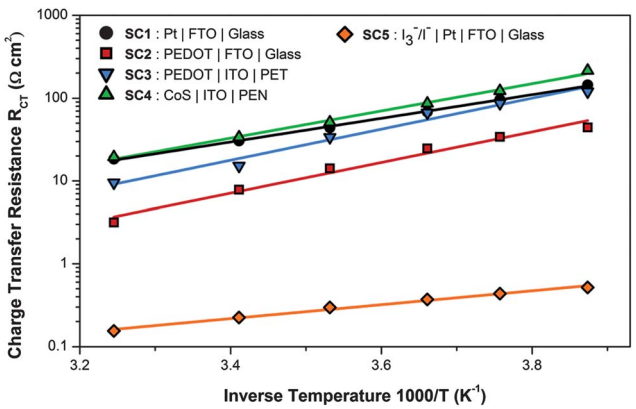

Fig. 4 Arrhenius plot of the charge transfer resistance. The charge transfer resistance is calculated as half the value obtained from the EIS fitting multiplied by the geometric surface area of the corresponding cell.

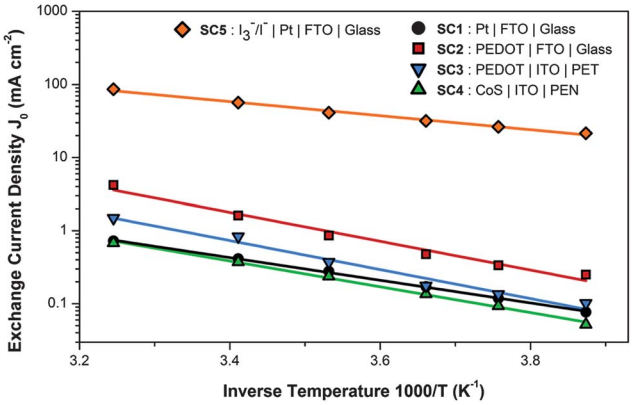

Fig. 5 Arrhenius plot of the exchange current density.

E_a for the electron transfer process at the counter electrode interface (Table 2).

It is known that platinum shows good catalytic activity for triiodide-to-iodide reduction, which agrees with the obtained low value for the apparent activation energy of 18.4 kJ mol^{-1}. In the case of the disulfide/thiolate redox electrolyte, platinum yields an apparent activation energy of 30.9 kJ mol^{-1}. As expected, similar results were obtained for the two PEDOT electrodes on different substrates, having values for PEDOT|FTO|Glass and PEDOT|ITO|PET of 37.8 kJ mol^{-1} and 38.1 kJ mol^{-1}, respectively. However, these activation energies are significantly higher than in the case of the conventional I_3^-/I^-|Pt system. The value extracted for CoS is 33.8 kJ mol^{-1}, which lies in-between the activation energy values of the Pt and PEDOT systems. It is interesting to note that the change of the electrocatalyst generally has only a little influence on the apparent activation energy for the electron transfer.

When comparing the different counter electrodes, it has to be considered that the area normalization only refers to the geometry of the symmetrical cell but does not take into consideration the surface area of the electroactive material on the counter electrode. Information on the electrocatalytic activity of the material can still be obtained, as the apparent activation energy is extracted from the slope of the Arrhenius plot.

3.3 Investigation of film morphology

The variation in photovoltaic performance as well as the results obtained by EIS can be further understood by considering the morphology of the different counter electrode materials that has been investigated by scanning electron microscopy (SEM). Standard platinum counter electrodes were prepared by thermal decomposition of H_2PtCl_6, a procedure that results in the formation of small nanoparticles and a final film thickness of only a few nanometres.[30] Consequently, the platinized counter electrode's surface roughness is determined by the roughness of the FTO glass substrate. However, the Pt nanoparticle film cannot be made visible by SEM, for which reason only the structure of FTO can be seen in Fig. 6a. By contrast, the use of hydrophobic ionic liquid as a medium for the EDOT electropolymerization leads to a nanoporous structured film with high surface area (Fig. 6g and h). Whilst in the case of FTO glass, the electrode's surface is uniformly coated with the polymer, the PEDOT film on ITO|PET is inhomogeneous and the TCO not completely covered (Fig. 6e and f). As both electrodes were prepared under identical conditions, this inhomogeneity is likely to result from a poor quality of the conductive TCO layer on the PET sheet, possibly arising from cracks that form due to bending of the flexible substrate during electrode fabrication. However, this can explain the lower fill factor and relatively high charge transfer resistance obtained for the flexible PEDOT electrode compared to PEDOT on FTO glass. Although it is difficult to elucidate the morphology of the CoS film by SEM (Fig. 6c and d), the images show that the TCO is not fully covered with the wrinkle-like nanoparticulate CoS structure. This is clearly evident when we compare the CoS coated counter electrode to the bare ITO|PEN substrate (Fig. 6b).

Together with the results obtained from EIS measurements, these findings demonstrate that the excellent performance of the PEDOT|FTO|Glass counter electrode results from the higher surface area of the PEDOT layer. This high surface area translates into a high electrocatalytic activity of the prepared electrode, which allows in compensating the slow electron transfer from the electrode to the disulfide species, rendering high fill factors possible.

3.4 Photovoltaic performance using the volatile electrolyte

As it is a well-known fact that the photovoltaic device performance strongly depends on the viscosity of the redox electrolyte, the PEDOT|FTO|Glass counter electrode has also been tested using an optimized volatile electrolyte. Under full sun illumination, a remarkable power conversion efficiency of 7.9% was achieved with J_{SC}, V_{OC} and FF values of 15.9 mA cm^{-2}, 687 mV and 0.72, respectively, as derived from J–V characteristics shown in Fig. 7a. Table 3 gives the detailed photovoltaic parameters at different light intensities. The incident photon-to-current conversion efficiency (IPCE) spectrum reaches a maximum of over 90% at 550 nm, whereas the J_{SC} value obtained from integrating the product of the IPCE spectrum with the AM1.5G spectral solar photon flux was close to the measured value (Fig. 7b).

3.5 Device stability

Despite the good performance of the iodine-free T_2/T^--based redox electrolyte, the long-term stability of photovoltaic cells still

Table 2 Apparent activation energies derived from the Arrhenius plot (Fig. 5). The activation energies were calculated according to the Arrhenius equation (eqn (2)) from the slope of linear fits (solid straight lines in Fig. 5)

	SC1 Pt|FTO|Glass	SC2 PEDOT|FTO|Glass	SC3 PEDOT|ITO|PET	SC4 CoS|ITO|PEN	SC5 I_3^-/I^-|Pt|FTO|Glass
E_a/kJ mol^{-1}	30.9	37.8	38.1	33.8	18.4

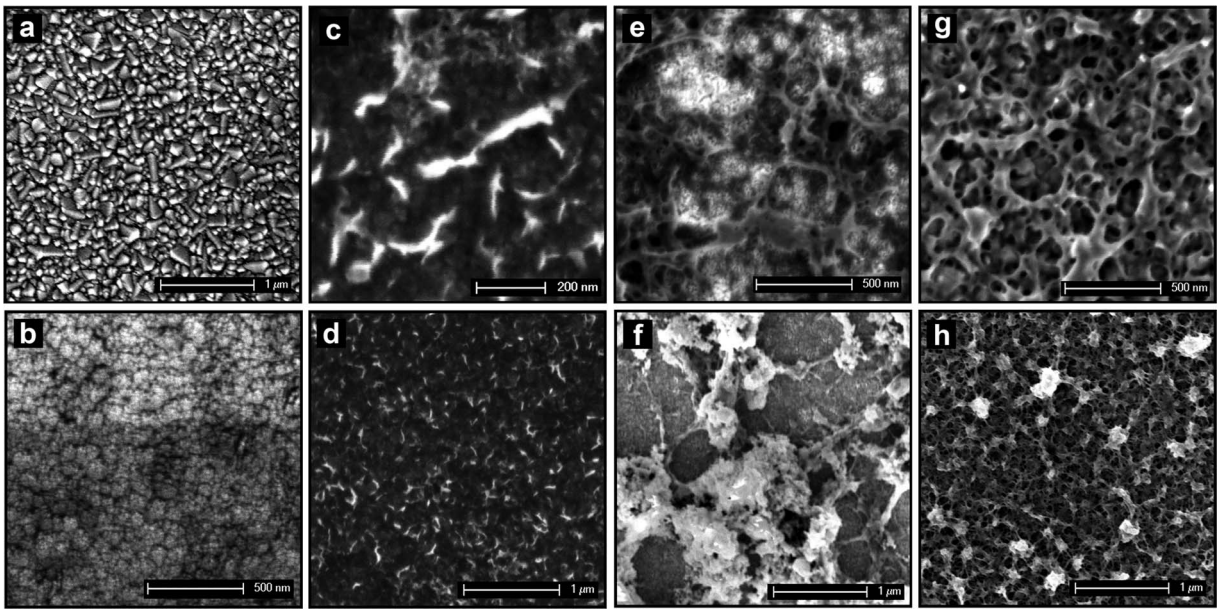

Fig. 6 Scanning Electron Microscopy (SEM) images of different counter electrodes: (a) Pt on FTO|Glass, (b) bare ITO|PEN, (c)/(d) CoS on ITO|PEN, (e)/(f) PEDOT on ITO|PET, and (g)/(h) PEDOT on FTO|Glass.

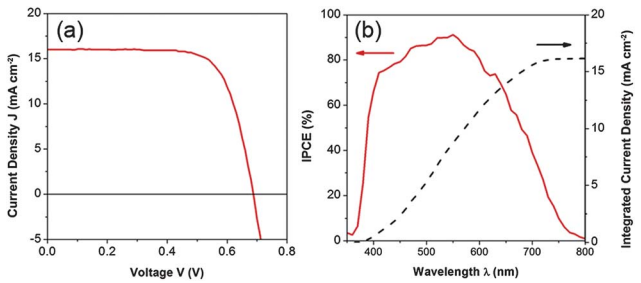

Fig. 7 (a) Measured *J–V* characteristics of a DSC employing the PEDOT|FTO|Glass counter electrode and a volatile electrolyte under 100 mW cm^{-2} illumination. The electrolyte composition is 0.3 M T_2 and 0.9 M T^- in a mixture of acetonitrile/ethylene carbonate in a 6 : 4 volume ratio. (b) The internal photon-to-electron conversion efficiency (IPCE) as a function of wavelength of monochromatic light. The right ordinate shows the integrated current density expected to be generated under standard illumination conditions (AM1.5G, 100 mW cm^{-2}).

Table 3 Photovoltaic parameters measured at different light intensities (AM1.5G Standard) for the PEDOT|FTO|Glass counter electrode and a volatile electrolyte

Intensity/mW cm^{-2}	10	50	100
V_{OC}/mV	622	670	687
J_{SC}/mA cm^{-2}	1.6	8.1	15.9
FF	0.78	0.76	0.72
η (%)	7.9	8.1	7.9

needs to be improved. Devices assembled with platinum-loaded counter electrodes suffer a quick decrease in power conversion efficiency, mainly due to short-circuit current density and fill factor losses (Fig. 8). A possible reason for this behaviour is the deactivation of the electroactive platinum layer on the counter electrode with time. It is well known that the sulfur-functionalized organic compounds such as thiols, thiolates or disulfides readily adsorb on noble metal surfaces forming self-assembled monolayers.[31] Moreover, platinum has already been proved inappropriate as electrocatalyst for the polysulfide redox couple S_n^{2-}/S_{n+1}^{2-} being widely used in quantum-dot-sensitized solar cells (QDSS) whereas materials like cobalt(II)sulfide, copper(I)sulfide or lead(II)sulfide showed much better electrocatalytic activity.[32,33]

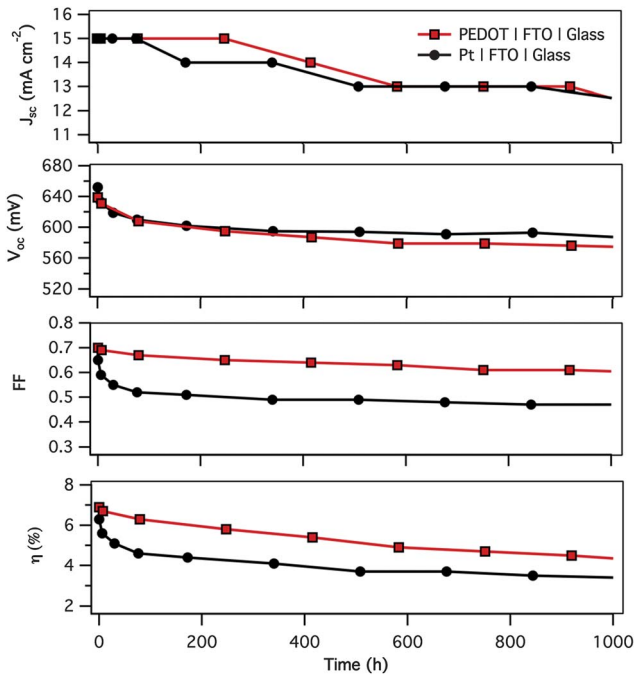

Fig. 8 Evolution of photovoltaic parameters for devices stored in the dark at ambient temperature (25 °C). *J–V* characteristics were measured weekly under standard solar conditions (AM1.5G, 100 mW cm^{-2}).

The stability of DSCs fabricated with the T_2/T^- redox couple could be significantly improved by replacing the thermalized platinum layer on the counter electrode by electrochemically deposited PEDOT. Devices employing the above mentioned PEDOT|FTO|Glass electrode maintained about 50% of their initial performance after 1000 hours when being stored in the dark at 25 °C (Fig. 8). However, preliminary studies show that the power conversion efficiency drops below 20% of the initial value within one week when the devices are subjected to standard light soaking conditions at 60 °C and full sunlight due to a drop of all photovoltaic parameters J_{SC}, V_{OC} and FF (data not shown). The performed stability tests at room temperature indicate that an additional degradation mechanism that is independent from the counter electrode seems to occur, as the initial drops of current and potential do not differ for both counter electrode materials. To understand the cause of this instability with the new promising T_2/T^- redox electrolyte, a detailed investigation is warranted.

4. Conclusions

We herein report on the successful introduction of two alternative platinum-free counter electrodes based on PEDOT and CoS in nanocrystalline DSCs employing an organic disulfide/thiolate redox couple. By using PEDOT electrochemically grown in ionic liquid, we could remarkably improve the performance as well as the stability of photovoltaic devices, reaching an unprecedented power conversion efficiency of 7.9% under standard solar conditions. The excellent photovoltaic performance clearly originates from the nanoporous structure and high surface area of the PEDOT electrode. Together with the transparent and non-corrosive disulfide/thiolate redox shuttle, the reported system shows great potential for practical large-scale application in DSCs. Long-term stability of photovoltaic devices remains as the major drawback of the presented system. However, the reason for the device instability is still unclear and further in-depth studies are required to elucidate this phenomenon. With the use of CoS, comparable results could be obtained under low light conditions, though the fill factor at full sun was rather poor. Nevertheless, we expect that the device performance could be significantly improved by increasing the surface area and quality of the deposited CoS films.

Acknowledgements

The authors thank P. Comte for TiO_2 film preparation, L.-P. Heiniger for recording SEM images and M. Wang and T. Moehl for helpful discussions. Financial support from the Swiss National Science Foundation and the National Sciences and Engineering Research Council of Canada (NSERC) is gratefully acknowledged. SA thanks Prof. H.-J. Butt and the Alexander Von Humboldt Foundation for their support. MG acknowledges the European Research Council (ERC) for an Advanced Research Grant (ARG no. 247404) funded under the "Meso-light" project.

Notes and references

1 M. Grätzel, Solar energy conversion by dye-sensitized photovoltaic cells, *Inorg. Chem.*, 2005, **44**, 6841–6851.
2 B. O'Regan and M. Grätzel, A low-cost, high-efficiency solar cell based on dye-sensitized colloidal TiO_2 films, *Nature*, 1991, **353**, 737–740.
3 G. Boschloo and A. Hagfeldt, Characteristics of the iodide/triiodide redox mediator in dye-sensitized solar cells, *Acc. Chem. Res.*, 2009, **42**, 1819–1826.
4 (*a*) Z.-S. Wang, K. Sayama and H. Sugihara, Efficient eosin Y dye-sensitized solar cell containing Br^-/Br_3^- electrolyte, *J. Phys. Chem. B*, 2005, **109**, 22449–22455; (*b*) H. Nusbaumer, J.-E. Moser, S. M. Zakeeruddin, M. K. Nazeeruddin and M. Grätzel, $CoII(dbbip)_2^{2+}$ complex rivals tri-iodide/iodide redox mediator in dye-sensitized photovoltaic cells, *J. Phys. Chem. B*, 2001, **105**, 10461–10464; (*c*) G. Oskam, B. V. Bergeron, G. J. Meyer and P. C. Searson, Pseudohalogens for dye-sensitized TiO_2 photoelectrochemical cells, *J. Phys. Chem. B*, 2001, **105**, 6867–6873; (*d*) Z. Zhang, P. Chen, T. Murakami, S. M. Zakeeruddin and M. Grätzel, The 2,2,6,6-tetramethyl-1-piperidinyloxy radical: an efficient, iodine-free redox mediator for dye-sensitized solar cells, *Adv. Funct. Mater.*, 2008, **18**, 341–346.
5 (*a*) S. M. Feldt, E. A. Gibson, E. Gabrielsson, L. Sun, G. Boschloo and A. Hagfeldt, Design of organic dyes and cobalt polypyridine redox mediators for high-efficiency dye-sensitized solar cells, *J. Am. Chem. Soc.*, 2010, **132**, 16714–16724; (*b*) H. N. Tsao, C. Yi, T. Moehl, J.-H. Yum, S. M. Zakeeruddin, M. K. Nazeeruddin and M. Grätzel, Cyclopentadithiophene bridged donor–acceptor dyes achieve high power conversion efficiencies in dye-sensitized solar cells based on the tris-cobalt bipyridine redox couple, *ChemSusChem*, 2011, **4**, 591–594.
6 T. Daeneke, T.-H. Kwon, A. B. Holmes, N. W. Duffy, U. Bach and L. Spiccia, High-efficiency dye-sensitized solar cells with ferrocene-based electrolytes, *Nat. Chem.*, 2011, **3**, 213–215.
7 M. Wang, N. Chamberland, L. Breau, J.-E. Moser, R. Humphry-Baker, B. Marsan, S. M. Zakeeruddin and M. Grätzel, An organic redox electrolyte to rival triiodide/iodide in dye-sensitized solar cells, *Nat. Chem.*, 2010, **2**, 385–389.
8 H. Tian, X. Jiang, Z. Yu, L. Kloo, A. Hagfeldt and L. Sun, Efficient organic-dye-sensitized solar cells based on an iodine-free electrolyte, *Angew. Chem., Int. Ed.*, 2010, **49**, 7328–7331.
9 (*a*) D. Li, H. Li, Y. Luo, K. Li, Q. Meng, M. Armand and L. Chen, Non-corrosive, non-absorbing organic redox couple for dye-sensitized solar cells, *Adv. Funct. Mater.*, 2010, **20**, 3358–3365; (*b*) Y. Liu, J. R. Jennings, M. Parameswaran and Q. Wang, An organic redox mediator for dye-sensitized solar cells with near unity quantum efficiency, *Energy Environ. Sci.*, 2011, **4**, 564–571.
10 M. Wu, Y. Wang, X. Lin, N. Yu, L. Wang, A. Hagfeldt and T. Ma, Economical and effective sulfide catalysts for dye-sensitized solar cells as counter electrodes, *Phys. Chem. Chem. Phys.*, 2011, **13**, 19298–19301.
11 N. Koide, A. Islam, Y. Chiba and L. Han, Improvement of efficiency of dye-sensitized solar cells based on analysis of equivalent circuit, *J. Photochem. Photobiol., A*, 2006, **182**, 296–305.
12 A. Kay and M. Grätzel, Low cost photovoltaic modules based on dye sensitized nanocrystalline titanium dioxide andcarbon powder, *Sol. Energy Mater. Sol. Cells*, 1996, **44**, 99–117.
13 T. N. Murakami, S. Ito, Q. Wang, M. K. Nazeeruddin, T. Bessho, I. Cesar, P. Liska, R. Humphry-Baker, P. Comte, P. Pechy and M. Grätzel, Highly efficient dye-sensitized solar cells based on carbon black counter electrodes, *J. Electrochem. Soc.*, 2006, **153**, A2255–2261.
14 (*a*) K. Suzuki, M. Yamaguchi, M. Kumagai and S. Yanagida, Application of carbon nanotubes to counter electrodes of dye-sensitized solar cells, *Chem. Lett.*, 2003, **32**, 28–29; (*b*) I. S. Cha, B. K. Koo, S. H. Seo and D. Y. Lee, Pt-free transparent counter electrodes for dye-sensitized solar cells prepared from carbon nanotube micro-balls, *J. Mater. Chem.*, 2010, **20**, 659–662.
15 (*a*) J. D. Roy-Mayhew, D. J. Bozym, C. Punckt and I. A. Aksay, Functionalized graphene as a catalytic counter electrode in dye-sensitized solar cells, *ACS Nano*, 2010, **4**, 6203–6211; (*b*) L. Kavan, J.-H. Yum and M. Grätzel, Optically transparent cathode for dye-sensitized solar cells based on graphene nanoplatelets, *ACS Nano*, 2011, **5**, 165–172.
16 (*a*) M. Wang, A. M. Anghel, B. Marsan, N.-L. Cevey Ha, N. Pootrakulchote, S. M. Zakeeruddin and M. Grätzel, CoS supersedes Pt as efficient electrocatalyst for triiodide reduction in dye-sensitized solar cells, *J. Am. Chem. Soc.*, 2009, **131**,

15976–15977; (*b*) H. Sun, D. Qin, S. Huang, X. Guo, D. Li, Y. Luo and Q. Meng, Dye-sensitized solar cells with NiS counter electrodes electrodeposited by a potential reversal technique, *Energy Environ. Sci.*, 2011, **4**(8), 2630–2637.

17 (*a*) Q. W. Jiang, G. R. Li and X. P. Gao, Highly ordered TiN nanotube arrays as counter electrodes for dye-sensitized solar cells, *Chem. Commun.*, 2009, 6720–6722; (*b*) G. R. Li, J. Song, G. L. Pan and X. P. Gao, Highly Pt-like electrocatalytic activity of transition metal nitrides for dye-sensitized solar cells, *Energy Environ. Sci.*, 2011, **4**, 1680–1683.

18 M. Wu, X. Lin, A. Hagfeldt and T. Ma, Low-cost molybdenum carbide and tungsten carbide counter electrodes for dye-sensitized solar cells, *Angew. Chem., Int. Ed.*, 2011, **50**, 3520–3524.

19 (*a*) Z. Li, B. Ye, X. Hu, X. Ma, X. Zhang and Y. Deng, Facile electropolymerized-PANI as counter electrode for low cost dye-sensitized solar cell, *Electrochem. Commun.*, 2009, **11**, 1768–1771; (*b*) Q. Tai, B. Chen, F. Guo, S. Xu, H. Hu, B. Sebo and X.-Z. Zhao, *In situ* prepared transparent polyaniline electrode and its application in bifacial dye-sensitized solar cells, *ACS Nano*, 2011, **5**, 3795–3799.

20 (*a*) J. Wu, Q. Li, L. Fan, Z. Lan, P. Li, J. Lin and S. Hao, High-performance polypyrrole nanoparticles counter electrode for dye-sensitized solar cells, *J. Power Sources*, 2008, **181**(1), 172–176; (*b*) J. Xia, L. Chen and S. Yanagida, Application of polypyrrole as a counter electrode for a dye-sensitized solar cell, *J. Mater. Chem.*, 2011, **21**, 4644.

21 (*a*) J.-G. Chen, H.-Y. Wei and K.-C. Ho, Using modified poly(3,4 ethylenedioxythiophene):poly(styrene sulfonate) film as a counter electrode in dye-sensitized solar cells, *Sol. Energy Mater. Sol. Cells*, 2007, **91**, 1472–1477; (*b*) K.-M. Lee, W.-H. Chiu, H.-Y. Wei, C.-W. Hu, V. Suryanarayanan, W.-F. Hsieh and K.-C. Ho, Effects of mesoscopic poly(3,4-ethylenedioxythiophene) films as counter electrodes for dye-sensitized solar cells, *Thin Solid Films*, 2010, **518**, 1716–1721; (*c*) J. M. Pringle, V. Armel and D. R. MacFarlane, Electrodeposited PEDOT-on-plastic cathodes for dye-sensitized solar cells, *Chem. Commun.*, 2010, **46**, 5367–5369.

22 L. Groenendaal, F. Jonas, D. Freitag, H. Pielartzik and J. R. Reynolds, Poly(3,4-ethylenedioxythiophene) and its derivatives: past, present and future, *Adv. Mater.*, 2000, **12**, 481–494.

23 S. Kirchmeyer and K. Reuter, Scientific importance, properties and growing applications of poly(3,4-ethylenedioxythiophene), *J. Mater. Chem.*, 2005, **15**, 2077–2088.

24 (*a*) S. Ahmad, J.-H. Yum, Z. Xianxi, M. Grätzel, H.-J. Butt and M. K. Nazeeruddin, Dye-sensitized solar cells based on poly (3,4-ethylenedioxythiophene) counter electrode derived from ionic liquids, *J. Mater. Chem.*, 2010, **20**, 1654–1658; (*b*) S. Ahmad, J.-H. Yum, H.-J. Butt, M. K. Nazeeruddin and M. Grätzel, Efficient platinum-free counter electrodes for dye-sensitized solar cell applications, *ChemPhysChem*, 2010, **11**, 2814–2819.

25 S. Ahmad, M. Deepa and S. Singh, Electrochemical synthesis and surface characterization of poly(3,4-ethylenedioxythiophene) films grown in an ionic liquid, *Langmuir*, 2007, **23**, 11430–11433.

26 H. Tian, Z. Yu, A. Hagfeldt, L. Kloo and L. Sun, Organic redox couples and organic counter electrode for efficient organic dye-sensitized solar cells, *J. Am. Chem. Soc.*, 2011, **133**(24), 9413–9422.

27 P. Wang, B. Wenger, R. Humphry-Baker, J.-E. Moser, J. Teuscher, W. Kantlehner, J. Mezger, E. V. Stoyanov, S. M. Zakeeruddin and M. Grätzel, Charge separation and efficient light energy conversion in sensitized mesoscopic solar cells based on binary ionic liquids, *J. Am. Chem. Soc.*, 2005, **127**, 6850–6856.

28 P. Bonhote, A.-P. Dias, N. Papageorgiou and K. Kalyanasundaram, Hydrophobic, highly conductive ambient-temperature molten salts, *Inorg. Chem.*, 1996, **35**, 1168–1178.

29 A. Hauch and A. Georg, Diffusion in the electrolyte and charge-transfer reaction at the platinum electrode in dye-sensitized solar cells, *Electrochim. Acta*, 2001, **46**, 3457–3466.

30 N. Papageorgiou, W. F. Maier and M. Grätzel, An iodine/triiodide reduction electrocatalyst for aqueous and organic media, *J. Electrochem. Soc.*, 1997, **144**, 876–884.

31 J. C. Love, L. A. Estroff, J. K. Kriebel, R. G. Nuzzo and G. M. Whitesides, Self-Assembled monolayers of thiolates on metals as a form of nanotechnology, *Chem. Rev.*, 2005, **105**, 1103–1169.

32 (*a*) S. Gimenez, I. Mora-Sero, L. Macor, N. Guijarro, T. Lana-Villarreal, R. Gomez, L. J. Diguna, Q. Shen, T. Toyoda and J. Bisquert, Improving the performance of colloidal quantum-dot-sensitized solar cells, *Nanotechnology*, 2009, **20**, 295204; (*b*) Z. Tachan, M. Shalom, I. Hod, S. Rühle, S. Tirosh and A. Zaban, PbS as a highly catalytic counter electrode for polysulfide-based quantum dot solar cells, *J. Phys. Chem. C*, 2011, **115**, 6162–6166.

33 G. Hodes, J. Manassen and D. Cahen, Electrocatalytic electrodes for the polysulfide redox system, *J. Electrochem. Soc.*, 1980, **127**, 544–549.